AN ENHANCED CONTROL STRATEGY OF THREE-PHASE FOUR-WIRE INVERTERS UNDER NONLINEAR LOAD CONDITIONS

Van Tan Luong[1]*, Pham Dinh Tiep[1], Le Nguyen Hoa Binh[2]

[1]*Ho Chi Minh City University of Food Industry*
[2]*Van Lang University*
*Email: *luongvt@hufi.edu.vn*

ABSTRACT

An enhanced nonlinear control technique based on a coordination between feedback linearization (FBL) approach and sliding mode control (SMC) is proposed for a three-phase split-capacitor inverter under the nonlinear load conditions. A nonlinear model of system with pulse-width modulation (PWM) voltage-source inverter (VSI) including the output inductor-capacitor (LC) filters is derived in the d-q-0 synchronous reference frame, not by small signal analysis. The controllers for d-q-0 components of three-phase line-to-neutral load voltages are designed by linear control theory. With the proposed coordination scheme, three-phase split-capacitor inverter provides an excellent control performance for regulating the load voltages with nearly zero steady-state errors in both the transient and steady states. The proposed scheme is verified by the simulation results which show that three-phase split-capacitor inverter gives a low total harmonic distortion (THD) for the load voltages under the balanced or unbalanced nonlinear load conditions.

Keywords: Nonlinear load, three-phase inverter, feedback linearization, sliding mode control, unbalanced load.

1. INTRODUCTION

Recently, three-phase inverter has been widely applied for standalone applications. These applications considered as loads could be the vehicles, trucks, or the photovoltaic power systems, and so on [1, 2]. These loads could be the three-phase loads and/or single-phase loads which can cause a three-phase unbalanced load, an irregularly distributed single-phase load or a balanced three-phase load operating at a fault condition. If the imbalanced loads appear in the system, the components of the unwanted negative-and zero-sequence currents are produced. The negative-sequence component of the currents can cause the excessive heating in machines, saturation of transformers and ripple in rectifiers. Meanwhile the zero-sequence currents cause excessive power losses in neutral lines and affect protection.

The three-phase inverter is connected to a load by a four-wire system, in which the neutral point of both source and load sides is also grounded. Several different methods have been applied to provide the neutral point of the source side. In the one way, the Δ/Y (delta/winding) transformer has been used, in which the Δ and Y windings are connected to the inverter and the load, respectively [3]. For this, the zero-sequence current is trapped in the Δ windings. However, the use of the transformer can make its topology bulky, heavy and costly. In the other ways, the three-phase split-capacitor inverters and the four-leg inverters equipped with

the eight switches have been employed. Nevertheless, the two switches must be required to add to the four-leg inverters and the three-dimension space vector modulation is so complicated [4]. Fortunately, a three-phase three-leg inverter with split direct current (DC) bus is one topology which can implement the three-phase four-wire system with a neutral point, as seen in the connection point of the load in Figure 1. Compared to a three-phase three-wire system, this topology can cope with the zero-sequence to regulate the output voltages to be balanced and the zero-sequence current can flow in the connection between the neutral point and the mid-point of the capacitive divider.

Several researches focusing on improving the quality of the output voltages for the inverters and uninterruptable power supply (UPS) have been suggested. A repetitive control is used to regulate the inverters for UPS applications, but this controller shows slow response and lack of systematical method to stabilize the dynamic error of the system [5, 6]. Although this method can obtain high performance of the output voltage, the techniques for the control design is relatively complicated. In [7], a control strategy applying the technique of the symmetrical sequence decomposition to extract the positive-, negative- and zero-sequence components from the unbalanced three-phase signals have been developed. The proportional-integral (PI) controllers for the current and voltage are used to regulate the output voltages of the inverter. However, the using of twelve PI controllers and the processes of the sequence decomposition and composition could increase the computation time. Also, this control strategy is only suitable for the case of unbalanced linear loads. Sliding-mode control techniques are applied for regulating the output voltages inverters [8, 9]. In [8], a good control performance is achieved in both unbalanced linear and nonlinear loads. However, it is not so easy to locate a satisfactory sliding mode surface. Also, the selected state feedback gains to stabilize the system must be carefully considered for the load variations and parameters uncertainties. In [9], the output voltage THDs which are shown in the experimental results is still high under the nonlinear load condition. In [10], a robust multivariable servomechanism control is employed to control three-phase inverters of a distributed generation system in standalone mode. This technique achieved a relatively good control performance, but it is complex and requires exact parameter values of an *RLC* load. Another control method using the nonlinear control with FBL method has been applied for the UPS as well as three-phase four-wire inverter [11-14]. In this method, the tracking controllers based on the PI regulators after linearizing the nonlinear model of the inverter including the output *LC* filters by the FBL technique was used to eliminate the steady-state errors. Under unbalanced and nonlinear load conditions, the FBL with PI tracking controllers fails to eliminate the steady-state errors completely due to appearance of the AC signals in the controlled variables.

To overcome the drawback of the above feedback linearization control method, an improved control strategy for the three-phase four-wire inverter is proposed in this paper, where a coordination of the FBL and the SMC is utilized. With this coordination, the nonlinear model of the three-phase four-wire inverter is linearized, which can work in the unbalanced and nonlinear load conditions well. Thus, the nonlinear controller designed becomes simpler and gives the fast performances of the system, compared with the PI voltage controllers. Simulation results for a three-phase four-wire inverter are provided to verify the validity of the proposed control scheme.
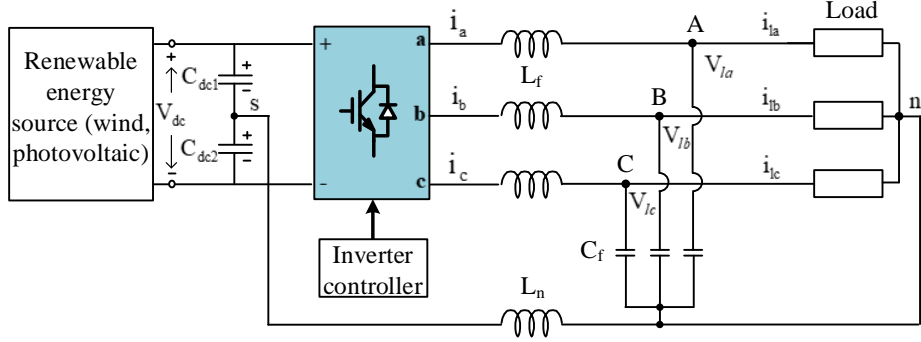
Figure 1. Circuit configuration of three-phase four-wire inverter.

2. SYSTEM MODELING

The three-phase split-capacitor inverter in Figure 1 can be represented in synchronous d-q-0 reference frame. Due to unbalanced load condition, the zero-sequence components are taken into account as

$$\dot{i}_{dq} = \frac{1}{L_f}v_{dq} - \frac{1}{L_f}v_{ldq} - j\omega i_{dq} \tag{1}$$

$$\dot{i}_0 = \frac{1}{\left(L_f + 3L_n\right)}v_0 - \frac{1}{\left(L_f + 3L_n\right)}v_{l0} \tag{2}$$

$$\dot{v}_{ldq} = \frac{1}{C_f}i_{dq} - \frac{1}{C_f}i_{ldq} - j\omega v_{ldq} \tag{3}$$

$$\dot{v}_{l0} = \frac{1}{C_f}i_0 - \frac{1}{C_f}i_{l0} \tag{4}$$

where L_f is the filter inductance, L_n is the neutral filter inductance, C_f is the filter capacitance, v_{dq} and v_0 are the d-q-0 axis inverter output voltages, v_{ldq} and v_{l0} are the d-q-0 axis phase load voltages, i_{dq} and i_0 are the d-q-0 axis inverter output currents, i_{ldq} and i_{l0} are the d-q-0 axis load currents, and ω is the source angle frequency.

From (1) to (3), a state-space modeling of the system is derived as follows:

$$
\begin{bmatrix} \dot{i}_d \\ \dot{i}_q \\ \dot{i}_0 \\ \dot{v}_{ld} \\ \dot{v}_{lq} \\ \dot{v}_{ln} \end{bmatrix}
=
\begin{bmatrix}
0 & \omega & 0 & -1/L_f & 0 & 0 \\
-\omega & 0 & 0 & 0 & -1/L_f & 0 \\
0 & 0 & 0 & 0 & 0 & -\frac{1}{L_f + 3L_n} \\
1/C_f & 0 & 0 & 0 & \omega & 0 \\
0 & 1/C_f & 0 & -\omega & 0 & 0 \\
0 & 0 & 1/C_f & 0 & 0 & 0
\end{bmatrix}
\begin{bmatrix} i_d \\ i_q \\ i_0 \\ v_{ld} \\ v_{lq} \\ v_{ln} \end{bmatrix}
+
\begin{bmatrix}
1/L_f & 0 & 0 \\
0 & 1/L_f & 0 \\
0 & 0 & \frac{1}{L_f + 3L_n} \\
0 & 0 & 0 \\
0 & 0 & 0 \\
0 & 0 & 0
\end{bmatrix}
\begin{bmatrix} v_d \\ v_q \\ v_n \end{bmatrix}
+
\begin{bmatrix} 0 \\ 0 \\ 0 \\ -i_{ld}/C_f \\ -i_{lq}/C_f \\ -i_{ln}/C_f \end{bmatrix}
\tag{5}
$$

3. PROPOSED INVERTER CONTROL SCHEME

3.1. Feedback linearization control

In order to remove the nonlinearity in the modeled system, a multi-input multi-output feedback linearization method is suggested [15]. The multi-input multi-output system is considered as:

5

$$\dot{x} = f(x) + g(x) \cdot u \tag{6}$$

$$y = h(x) \tag{7}$$

where x is state vector, u is control input, y is output, f and $g(x)$ are smooth vector fields, h is smooth scalar function.

The dynamic model of the inverter in (5) is expressed in (6) and (7) as

$$x = \begin{bmatrix} i_d \\ i_q \\ i_0 \\ v_{ld} \\ v_{lq} \\ v_{l0} \end{bmatrix}; u = \begin{bmatrix} v_{ld} \\ v_{lq} \\ v_{l0} \end{bmatrix}; y = \begin{bmatrix} v_d \\ v_q \\ v_0 \end{bmatrix}$$

To generate an explicit relationship between the outputs $y_{i=1,2,3}$ and the inputs $u_{i=1,2,3}$, each output $y_{i=1,2,3}$ is differentiated until a control input appears.

$$\begin{bmatrix} \ddot{y}_1 \\ \ddot{y}_2 \\ \ddot{y}_3 \end{bmatrix} = F(x) + G(x) \begin{bmatrix} u_1 \\ u_2 \\ u_3 \end{bmatrix} \tag{8}$$

Then, the control law is given as

$$\begin{bmatrix} v_d^* \\ v_q^* \\ v_0^* \end{bmatrix} = \begin{bmatrix} u_1 \\ u_2 \\ u_3 \end{bmatrix} = G^{-1}(x) \left[-F(x) + \begin{bmatrix} z_1 \\ z_2 \\ z_3 \end{bmatrix} \right] \tag{9}$$

where

$$F(x) = \begin{bmatrix} \dfrac{1}{C_f} 2\omega i_q - \left(\dfrac{1}{L_f C_f} + \omega^2 \right) v_{ld} - \dfrac{1}{C_f} \dot{i}_{ld} - \dfrac{1}{C_f} \omega i_q \\ -\dfrac{1}{C_f} 2\omega i_d - \left(\dfrac{1}{L_f C_f} + \omega^2 \right) v_{lq} - \dfrac{1}{C_f} \dot{i}_{lq} + \dfrac{1}{C_f} \omega i_d \\ -\dfrac{1}{\left(L_f + 3L_n \right) C_f} v_{l0} - \dfrac{1}{C_f} \dot{i}_{l0} \end{bmatrix}; \quad G(x) = \begin{bmatrix} \dfrac{1}{L_f C_f} & 0 & 0 \\ 0 & \dfrac{1}{L_f C_f} & 0 \\ 0 & 0 & \dfrac{1}{\left(L_f + 3L_n \right) C_f} \end{bmatrix}$$

and z_1, z_2 and z_3 are new control inputs.

A desired dynamic response can be imposed to the system by selecting

$$\begin{bmatrix} z_1 \\ z_2 \\ z_3 \end{bmatrix} = \begin{bmatrix} \ddot{y}_1^* + \alpha_{11}\dot{e}_1 + \alpha_{12}e_1 \\ \ddot{y}_2^* + \alpha_{21}\dot{e}_2 + \alpha_{22}e_2 \\ \ddot{y}_3^* + \alpha_{31}\dot{e}_3 + \alpha_{32}e_3 \end{bmatrix} \tag{10}$$

where $e_1 = y_1^* - y_1$, $e_2 = y_2^* - y_2$ and $e_3 = y_3^* - y_3$. y_1^*, y_2^* and y_3^* are the reference values of the y_1, y_2 and y_3, respectively.

The following error dynamics in Laplace domains can be formulated from (10) as

$$s^2 + \alpha_{11}s + \alpha_{12} = 0$$
$$s^2 + \alpha_{21}s + \alpha_{22} = 0 \qquad (11)$$
$$s^2 + \alpha_{31}s + \alpha_{32} = 0$$

which are stable if the gains α_{11}, α_{12}, α_{21}, α_{22}, α_{31}, and α_{32} are positive [11].

To have an exact idea of the controller complexity, the control inputs of (8) can be formulated separately as

$$u_1 = z_1 L_f C_f - 2\omega L_f i_q + \left(1 + \omega^2 L_f C_f\right)v_{ld} + L_f \dot{i}_{ld} + \omega L_f i_q$$
$$u_2 = z_2 L_f C_f + 2\omega L_f i_d + \left(1 + \omega^2 L_f C_f\right)v_{lq} + L_f \dot{i}_{lq} - \omega L_f i_d \qquad (12)$$
$$u_3 = z_3 L_f C_f + \frac{1}{\left(L_f + 3L_n\right)}L_f v_{l0} + L_f \dot{i}_{l0}$$

As can be seen from (12), it is not easy to implement the linearized voltages (v_{ld}, v_{lq}, v_{l0}), since they contain the time derivative components of currents (i_{ld}, i_{lq}, i_{l0}). Thus, a controller based on sliding mode is suggested, so that an input–output of the system controller is linearized and can be implemented with a digital method for convenience.

3.2. Sliding mode input-output feedback linearization control

The sliding surfaces with the errors of the indirect component voltages are expressed as [15]:

$$s_1 = \dot{e}_1 + \alpha_{11}e_1 + \alpha_{12}\int e_1 dt$$
$$s_2 = \dot{e}_2 + \alpha_{21}e_2 + \alpha_{22}\int e_2 dt \qquad (13)$$
$$s_3 = \dot{e}_3 + \alpha_{31}e_3 + \alpha_{32}\int e_3 dt$$

If the system states operate on the sliding surface, then $s_1 = s_2 = s_3 = 0$ and $\dot{s}_1 = \dot{s}_2 = \dot{s}_3 = 0$. Substituting (13) into $\dot{s}_1 = \dot{s}_2 = \dot{s}_3 = 0$ yields

$$\ddot{e}_1 = -\alpha_{11}\dot{e}_1 - \alpha_{12}e_1; \quad \ddot{e}_2 = -\alpha_{21}\dot{e}_2 - \alpha_{22}e_2; \quad \ddot{e}_3 = -\alpha_{31}\dot{e}_3 - \alpha_{32}e_3 \qquad (14)$$

It is guaranteed in (14) that the system states (v_{ld}, v_{lq}, v_{l0}) will exponentially converge towards the reference values when they are kept the sliding surface to zero. The equivalent control concept of a sliding surface is the continuous control that allows the maintenance of the state trajectory on the sliding surface $s = \dot{s} = 0$. The equivalent control is achieved from (13) as

$$\dot{s}_1 = z_1 - \frac{2}{C_f}\omega i_q + \left(\frac{1}{L_f C_f} + \omega^2\right)v_{ld} + \frac{1}{C_f}\dot{i}_{ld} + \frac{1}{C_f}\omega i_q$$

$$\dot{s}_2 = z_2 + \frac{2}{C_f}\omega i_d + \left(\frac{1}{L_f C_f} + \omega^2\right)v_{lq} + \frac{1}{C_f}\dot{i}_{lq} - \frac{1}{C_f}\omega i_d \qquad (15)$$

$$\dot{s}_3 = z_3 + \frac{1}{\left(L_f + 3L_n\right)C_f}v_{l0} + \frac{1}{C_f}\dot{i}_{l0}$$

where z_1, z_2 and z_3 coincide with the new inputs of the system, whose expressions are

expressed as

$$z_1 = \ddot{v}_{ld}^* + \alpha_{11}\dot{e}_1 + \alpha_{12}e_1$$
$$z_2 = \ddot{v}_{lq}^* + \alpha_{21}\dot{e}_2 + \alpha_{22}e_2 \tag{16}$$
$$z_3 = \ddot{v}_{l0}^* + \alpha_{31}\dot{e}_3 + \alpha_{32}e_3$$

The equivalent control is obtained by making $\dot{s}_1 = \dot{s}_2 = \dot{s}_3 = 0$ as:

$$u_{1eq} = z_1 L_f C_f - 2\omega L_f i_q + \left(1 + \omega^2 L_f C_f\right)v_{ld} + L_f \dot{i}_{ld} + \omega L_f i_q$$

$$u_{2eq} = z_2 L_f C_f + 2\omega L_f i_d + \left(1 + \omega^2 L_f C_f\right)v_{lq} + L_f \dot{i}_{lq} - \omega L_f i_d \tag{17}$$

$$u_{3eq} = z_3 L_f C_f + \frac{1}{\left(L_f + 3L_n\right)} L_f v_{l0} + L_f \dot{i}_{l0}$$

The equivalent obtained control is similar to the one achieved in (12). In order to drive the state variables to the sliding surface $s_1 = s_2 = s_3 = 0$, in the case of $s_1, s_2, s_3 \neq 0$, the control laws are defined as

$$u_1 = u_{1eq} + u_{1st}$$
$$u_2 = u_{2eq} + u_{2st} \tag{18}$$
$$u_3 = u_{3eq} + u_{3st}$$

where $u_{1st} = \gamma_1 \operatorname{sign}(s_1)$, $u_{2st} = \gamma_2 \operatorname{sign}(s_2)$, $u_{3st} = \gamma_3 \operatorname{sign}(s_3)$, $\gamma_1 > 0, \gamma_2 > 0, \gamma_3 > 0$.
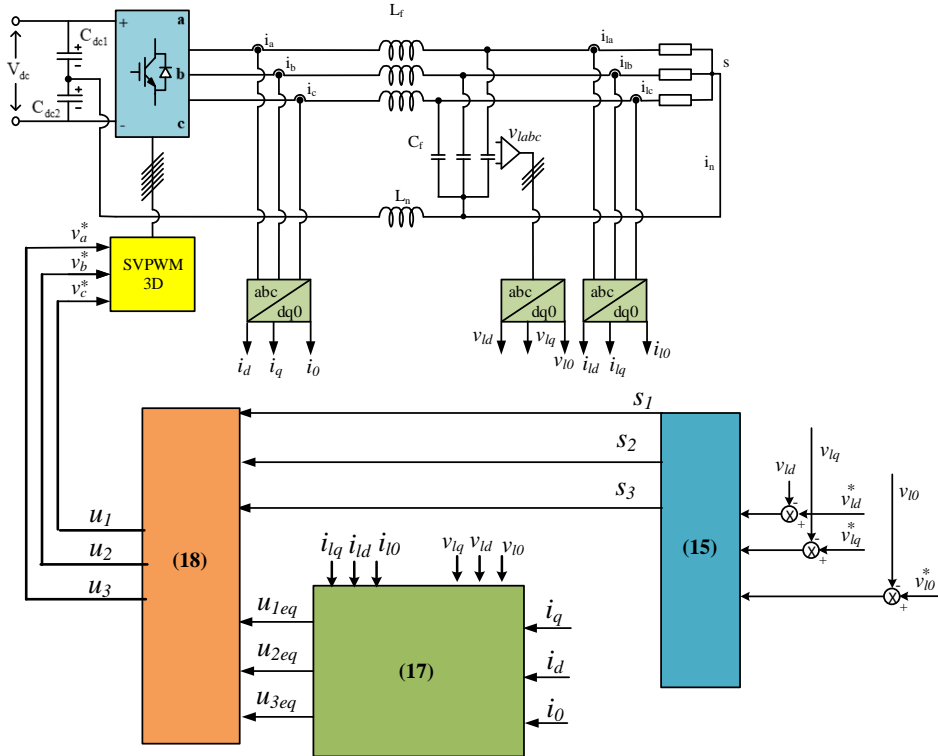

Figure 2. Block diagram of the proposed inverter control scheme.

The reaching law can be derived by substituting (17) and (18) into (15), which gives

$$\dot{s}_1 = -\gamma_1 \, sign(s_1); \;\; \dot{s}_2 = -\gamma_2 \, sign(s_2); \;\; \dot{s}_3 = -\gamma_3 \, sign(s_3) \tag{19}$$

The stability and robustness can be tested, using Lyapunov's function which is presented in [15].

Figure 2 shows the block diagram of the proposed controller, in which the dq0-axis load voltages use the sliding mode input-output feedback linearization control. The outputs of controller (v_a^*, v_b^*, v_c^*) are applied for SVPWM-3D (space vector pulse-width modulation - three dimensions).

4. SIMULATION RESULTS

To verify the feasibility of the proposed method, PSIM simulations have been carried out for the unbalanced and nonlinear loads. The DC-link voltage at the input of inverter from a three-phase ac source is 500 [V], the switching frequency of inverter is 10 [kHz]. The filter inductor L_f is 3 [mH] and the filter capacitor C_f is 100 [μF] which correspond to a cut-off frequency at 450 [Hz]. The parameters of loads and controllers are shown in the Table 1 and Table 2, respectively.

Table 1. Parameters of loads

Type of load	Parameters
Balanced nonlinear load	L_s = 1 [mH], C = 4.7 [mF], R_{dca} = R_{dcb} = R_{dcc} = 50 [Ω]
Unbalanced nonlinear load	L_s = 1 [mH], C = 4.7 [mF], R_{dca} = 50 [Ω], R_{dcb} = R_{dcc} = 1 [kΩ]

Table 2. Parameters of controllers

Controller type		Gain of controller	
		Balanced nonlinear load	Unbalanced nonlinear load
PI	Current controller	k_p = 5.4 k_i = 4000	k_p = 17.5 k_i = 13100
	Voltage controller	k_{pv} = 0.21 k_{iv} = 682	k_{pv} = 0.32 k_{iv} = 896
Proposed controller (FBL and SMC)		k_{11} = k_{21} = k_{31} = 5 × 10³, k_{12} = k_{22} = k_{32} = 8.4 × 10⁶	

Table 3. THD of load voltages

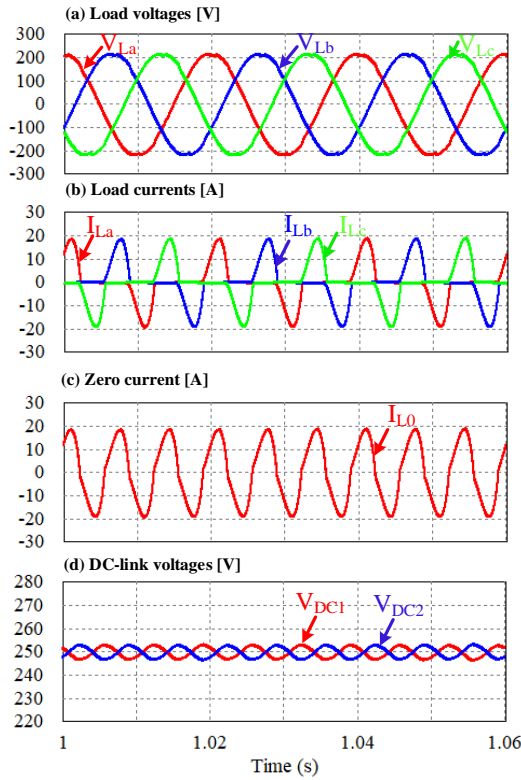| Load type	Controller type	THD [%]		
		THD (phase A)	THD (phase B)	THD (phase C)
Balanced nonlinear load	PI	2.14	0.58	0.45
	Proposed controller (FBL and SMC)	0.94	0.45	0.35
Unbalanced nonlinear load	PI	2.5	0.6	0.5
	Proposed controller (FBL and SMC)	1.05	0.38	0.39

Figure 3. Dynamic response of PI controller under the conditions of balanced nonlinear loads: (a) Load voltages, (b) Load currents, (c) Zero current, (d) DC-link voltages.
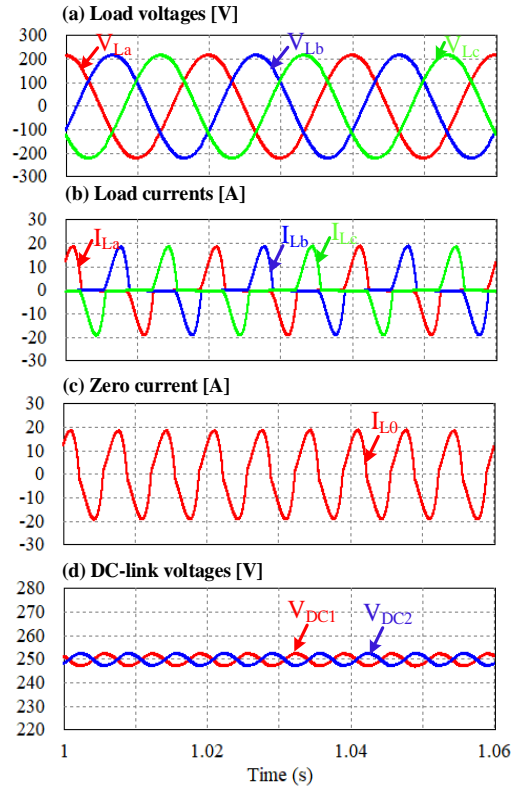
Figure 4. Dynamic response of proposed controller under the conditions of balanced nonlinear loads: (a) Load voltages, (b) Load currents, (c) Zero current, (d) DC-link voltages.

The simulation results for the system using the proposed controller and PI controller in the case of the balanced nonlinear loads are shown in Figures 3 and 4, respectively. Each illustration shows the load voltages (V_{LA}, V_{LB}, V_{LC}), load currents (I_{LA}, I_{LB}, I_{LC}), neutral current (I_{L0}) and voltages across two DC capacitors (V_{DC1}, V_{DC2}).

As can be clearly seen in Figures 3 and 4, the phase load voltages (Figures 3 (a) and 4(a)) become sinusoidal and are maintained at rated values under the balanced and nonlinear load conditions. However, the phase-A load voltage in the proposed controller is more almost sinusoidal, in the comparison with the traditional PI one. Also, the total harmonic distortion (THD) of the load voltage given in Table 3 shows that a THD of phase-A voltage in the case of using a PI controller is 2.14%, which is greater than that of using the proposed controller (0.94%).

The simulation results for the standalone inverter system using the proposed controller and the PI controller in case of unbalanced nonlinear loads are illustrated in Figures 5 and 6, respectively. By using the PI controller, the load voltages, load currents, neutral current and voltages across two DC capacitors are shown from Figure 5(a) to (d), respectively. Similarly, the load voltages, load currents, neutral current and voltages across two DC capacitors in the proposed controller are illustrated from Figure 6(a) to (d), respectively. Compared with the traditional PI controller, the load voltages in the proposed one as shown in Figure 6(a) give better performance. On the other hand, the load voltages in the proposed method are regulated to be rated and are almost sinusoidal.

In the case of an unbalanced nonlinear load, the THD (Table 3) of the phase-A load voltage using the PI controller is 2.5%, which is still greater than the proposed controller (1.05%).
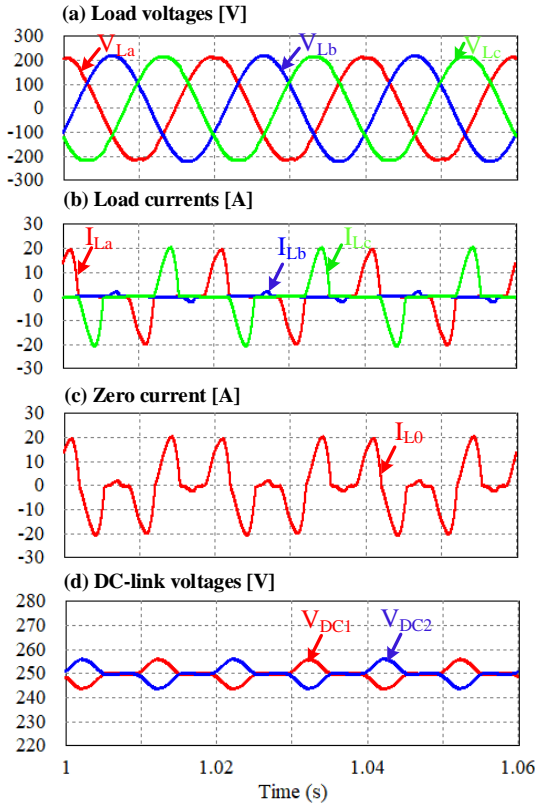

Figure 5. Dynamic response of PI controller under the conditions of unbalanced nonlinear loads: (a) Load voltages, (b) Load currents, (c) Zero current, (d) DC-link voltages.
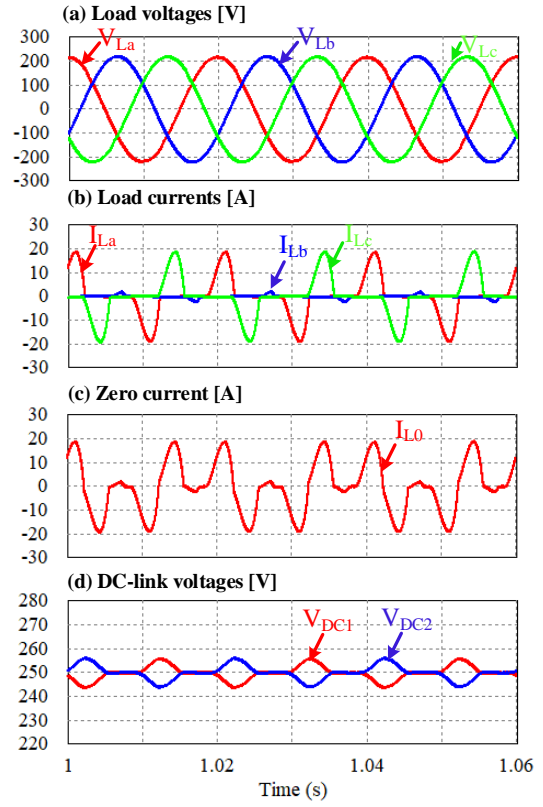
Figure 6. Dynamic response of proposed controller under the conditions of unbalanced nonlinear loads: (a) Load voltages, (b) Load currents, (c) Zero current, (d) DC-link voltages.
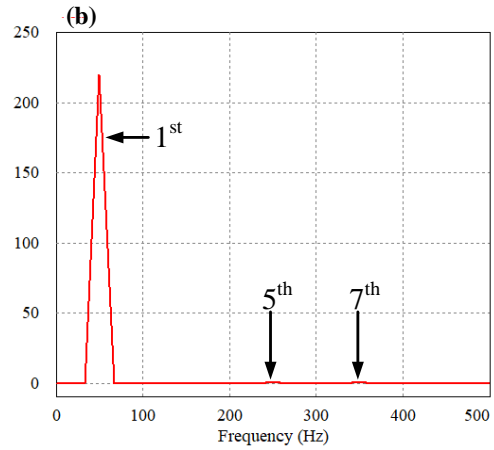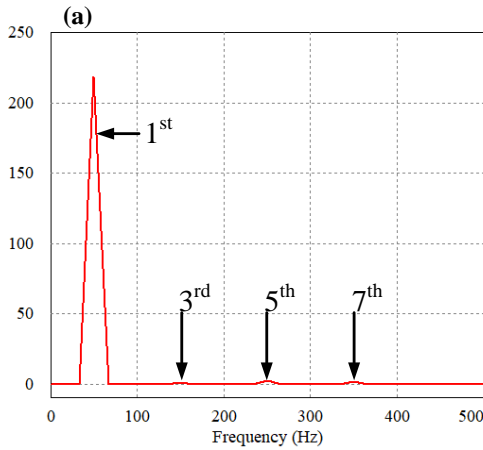

Figure 7. FFT spectra of the phase-A load voltage under the conditions of balanced nonlinear loads: (a) Using the PI controller, (b) Using the proposed controller.
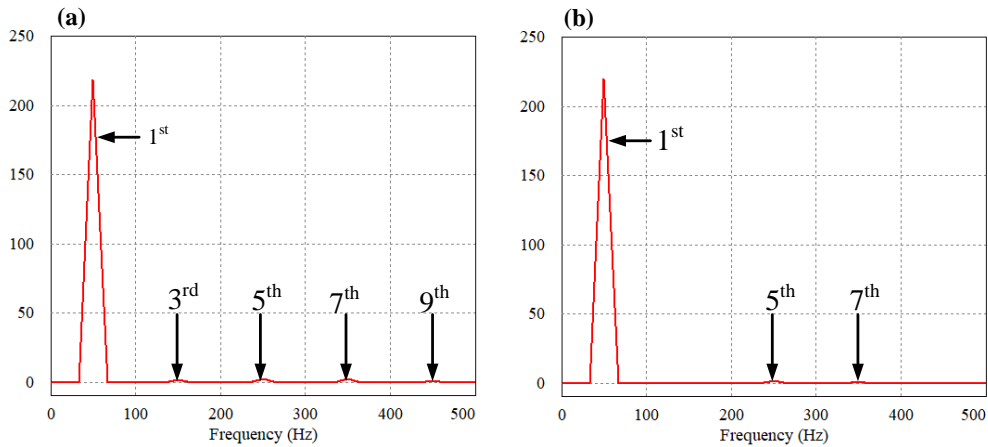
Figure 8. FFT spectra of the phase-A load voltage under the conditions of unbalanced nonlinear loads: (a) Using the PI controller, (b) Using the proposed controller.

To clarify the output voltage quality of the inverter, a fast Fourier transform (FFT) spectra analysis of the phase-A load voltage is performed in the two cases (balanced and unbalanced nonlinear loads), which are shown in Figures 7 and 8. In the case of using a PI controller, the load voltage in phase-A contains the high order frequency components such as 3rd, 5th, 7th (both cases) and 9th (just in case of unbalanced nonlinear loads) since the PI controller bandwidth does not respond to high frequencies well. In the case of using the proposed controller, the THD of the load voltage has been greatly reduced, compared to the case of using a PI controller. Specifically, the phase-A voltage no longer contains 3rd-order frequency components in the balanced nonlinear load conditions (Figure 7(b)) and 3rd and 9th-order frequency components in the unbalanced nonlinear load conditions (Figure 8(b)). Thus, it can be seen that the proposed control method achieves better performance than the PI controller in the cases of balanced nonlinear loads and unbalanced nonlinear loads.

5. CONCLUSION

The paper proposed a novel output voltage control of three-phase split-capacitor inverter based on the feedback-linearization technique and sliding mode control. This control method can regulate the load voltages in the case of unbalanced or unbalanced nonlinear loads. With this method, the load voltages are kept mostly balanced and sinusoidal with a low THD value for the simulation. The response of the three-phase split-capacitor inverter with the proposed strategy is better than the existing PI method. In the future, the proposed method can be used for unbalanced and distorted distribution grid voltage conditions.

REFERENCES

1. Jeung Y. C., Lee D. C. - AC power supply system using vehicle engine-generator set with battery, Proc. of IPEMC (ECCE-Asia) (2012) 1724-1728.

2. El-Barbari S., Hofmann W. - Digital control of a four leg inverter for standalone photovoltaic systems with unbalanced load, in Proc. of IEEE IECON (2000) 729-734.

3. Marwali M. N., Dai M. and Keyhani A. - Robust stability analysis of voltage and current control for distributed generation systems, IEEE Transactions on Energy Convers **21** (2) (2006) 516-526.

4. Zhang R., Prasad H., Boroyevich D., and Lee F. C. - Three-dimensional space vector modulation for four-leg voltage-source converters, IEEE Transactions on Power Electronics **17** (3) (2002) 314-326.

5. Haneyoshi T., Kawamura A. and Hoft R. G. - Waveform compensation of PWM inverter with cyclic fluctuating loads, IEEE Transactions on Industry Application **24** (4) (1988) 582-589.

6. Tzou Y. Y., Ou R. S., Jung S. L. and Chang M. Y. - High-performance programmable AC power source with low harmonic distortion using DSP-based repetitive control technique, IEEE Transactions on Power Electronics **12** (4) (1997) 715-725.

7. Mohd A., Ortjohann E., Hamsic N., Sinsukthavorn W., Lingemann M., Schmelter A., and Morton D. - Control strategy and space vector modulation for three-leg four-wire voltage source inverters under unbalanced load conditions, IET Power Electronics **3** (3) (2010) 323-333.

8. Zhang R., Boroyevich D., Prasad V. H., Mao H., Lee F. C., and Dubovsky S. - A three-phase inverter with a neutral leg with space vector modulation, in Proceedings of IEEE Applied Power Electronics Conference **2** (1997) 857-863.

9. Jung S. L. and Tzou Y. Y. - Discrete sliding-mode control of a PWM inverter for sinusoidal output waveform synthesis with optimal sliding curve, IEEE Transactions on Power Electronics **11** (4) (1996) 567-577.

10. Karimi H., Davison E. J., and Iravani R. - Multivariable servomechanism controller for autonomous operation of a distributed generation unit: Design and performance evaluation, IEEE Transactions on Power Systems **25** (2) (2010) 835-865.

11. Kim D-E, Lee D-C.- Feedback linearization control of three-phase UPS inverter system, IEEE Transactions on Industrial Electronics **57** (3) (2010) 963-968.

12. Vo N.Q.T., Lee D-C. - Advanced control of three-phase four-wire inverters using feedback linearization under unbalanced and nonlinear load condition, Transactions on Korean Institute of Power Electronics **18** (4) (2013) 333-341.

13. Jeong S.Y., Nguyen T.H., Le Q.A., Lee D.-C. - High-performance control of three-phase four-wire DVR systems using feedback linearization, Journal of Power Electronics **16** (1) (2016) 351-361.

14. Hosani K. A., Nguyen T. H., Sayari N. A. - An improved control strategy of 3P4W DVR systems under unbalanced and distorted voltage conditions, Electrical Power and Energy Systems **98** (2018) 233-242.

15. Slotine J.-J. E. and Li W.- Applied nonlinear control, Englewood Cliffs, NJ: Prentice-Hall (1991) 207-271.

TÓM TẮT

CHIẾN LƯỢC ĐIỀU KHIỂN NÂNG CAO CỦA BỘ NGHỊCH LƯU BA PHA BỐN DÂY TRONG TRƯỜNG HỢP TẢI PHI TUYẾN

Văn Tấn Lượng[1]*, Phạm Đình Tiệp[1], Lê Nguyễn Hòa Bình[2]
[1]Trường Đại học Công nghiệp Thực phẩm TP.HCM
[2]Trường Đại học Văn Lang
Email: luongvt@hufi.edu.vn

Kỹ thuật điều khiển phi tuyến nâng cao dựa trên sự phối hợp giữa kỹ thuật tuyến tính hóa hồi tiếp (FBL) và điều khiển trượt (SMC) được đề xuất cho bộ nghịch lưu chia tụ ba pha trong trường hợp tải phi tuyến. Mô hình phi tuyến của hệ thống với bộ nghịch lưu nguồn điện áp điều chế độ rộng xung (PWM) bao gồm các bộ lọc LC ở ngõ ra được hình thành trong hệ tọa độ quay (dq0), mà không cần dùng phương pháp phân tích tín hiệu nhỏ. Bộ điều khiển đối với các thành phần d-q-0 của điện áp pha của tải được thiết kế theo kỹ thuật điều khiển tuyến tính. Với chiến lược kết hợp đề xuất, bộ nghịch lưu chia tụ ba pha tạo ra vận hành điều khiển tốt để điều khiển điện áp tải với sai số gần như bằng không cả trạng thái quá độ và xác lập. Chiến lược đề xuất được kiểm chứng bởi các kết quả mô phỏng, cho thấy rằng bộ nghịch lưu chia tụ ba pha cho độ méo hài tổng (THD) thấp đối với điện áp tải trong trường hợp tải phi tuyến cân bằng và không cân bằng.

Từ khóa: Tải phi tuyến, bộ nghịch lưu ba pha, tuyến tính hóa hồi tiếp, điều khiển trượt, tải không cân bằng.